A HYBRID ACTIVE POWER FILTER CONNECTED TO A PHOTOVOLTAIC ARRAY

(Date received: 22.11.2007)

Zainal Salam[1], Tan Perng Cheng[2] and Awang Jusoh[3]

Power Electronics and Drives Group, Department of Energy Conversion, Faculty of Electrical Engineering, Universiti Teknologi Malaysia, 81310 UTM Skudai, Johor Bahru

Email: [1]zainals@fke.utm.my, [2]perngcheng@ieee.org, [3]awang@fke.utm.my

ABSTRACT

This paper presents a single-phase two-wire hybrid active power filter (APF) that is connected to photovoltaic (PV) array. The uniqueness of proposed scheme is the fact that it the combines the conventional APF with high-pass filter and PV. This approach improves the harmonics filtering performance as well as simultaneously supplies the power from the photovoltaic array to the load. The current reference command is derived using the extension instantaneous-reactive power (p-q) theorem. To prove the workability of the concept, an experimental APF system was designed and the proposed algorithm was tested.

Keywords: *Extension p-q Theorem, Hybrid Active Power Filter, Photovoltaic, Power Electronics*

1. INTRODUCTION

Due to the proliferation of nonlinear and switching loads from electrical power converters, such as thyristor/diode rectifiers, cycloconverters and arc furnaces, there is an increasing urgency to control and reduce the harmonics current in distribution power lines [1]. These types of loads draw harmonic currents from the mains, and if the supply impedance is sufficiently large, it can cause the supply voltage at the point of common coupling to be distorted. Harmonics have a number of undesirable effects on system. Short-term effects are usually the most noticeable – they are related to excessive voltage distortion. If the line inductance of the supply is large, there is a possibility of equipment failure due to excessive voltage distortion. On the other hand, long-term effects often go undetected and are usually related to increased resistive losses or voltage stresses. In addition, the harmonic currents produced by nonlinear loads can interact adversely with a wide range of power system equipment, most notably capacitors, transformers, and motors, causing additional losses, overheating, and overloading. These harmonic currents can also cause interferences with telecommunication lines and errors in metering devices.

Remarkable progress in power electronics switches technology and the availably of the fast processors such as the digital signal processor (DSP), microcontrollers and field programmable gate array (FPGA) had spurred interest in active power filter (APF) for harmonics mitigation [2–6]. The APF are superior in filtering performance, smaller in size and more flexible compared the traditional passive (power) filters. The basic principle of APF is to utilise power electronics technologies to produce harmonics current components that cancel the harmonics current components from the nonlinear loads. There are two types of active filters, namely the "pure" (or conventional) APF and the hybrid APF. The main advantage of the latter is the significant reduction in the power ratings of the APF [7]. The idea of hybrid APF using high pass passive filter (HPF) has been proposed by several researchers [8–10]. In this scheme, a low rating passive high-pass filter is used in addition to the pure APF. The harmonics filtering task is divided between the two filters. The APF cancels the lower order harmonics, while the HPF filters the higher order harmonics. The main objective of hybrid APF, therefore is to improve the filtering performance of high-order harmonics while providing a cost-effective low order harmonics mitigation.

In this paper, we propose a hybrid APF topology for a single-phase two-wire system, connected to a photovoltaic (PV) array. This topology is unique because it effectively filters harmonics current less than 1 kHz and of higher frequency. Furthermore, it simultaneously supplies the power from the PV array to the load and the distribution. This is a response to the increasing concern about the environment pollution. The need to generate pollution-free energy has triggers considerable interest toward renewable sources [11]. Efforts have been made to combine the APF with PV system [12–14]. However, it appears that no attempt has been made to combine a hybrid APF with PV system.

The main contribution of this work is the application of the extension instantaneous-reactive power (p-q) theorem to derive the compensation current reference for this topology. Although the derivation of current reference based on extension p-q theorem is not new [13–15], this approach has not yet being applied to a single-phase two-wire hybrid APF system involving passive high-pass filter (HPF), APF and PV array. Using the extension p-q theorem, the resulting equations for the reference current of single-phase two-wire system is simpler compared with the p-q theorem presented in [16]. This paper will primarily focus on the power circuit, the compensation current reference derivation, and the passive HPF design. Finally, the experimental test-rig (power rating of about 500W) is constructed that verify the theoretical predictions. Although the power rating of the experimental test-rig is not realistic for industrial use, it is quite sufficient to prove that the concept is workable.

II. PRINCIPLE OF OPERATION

Figure 1(a) presents the proposed hybrid APF with PV system block diagram, connected in parallel with a nonlinear load. It consists of a passive HPF, a single-phase APF constructed using a full-bridge voltage source inverter (VSI) and PV array. The VSI and the PV array are connected in parallel with the DC-bus capacitor. In the proposed scheme, the low-order harmonics are compensated using the shunt APF, while the high-order harmonics are filtered by

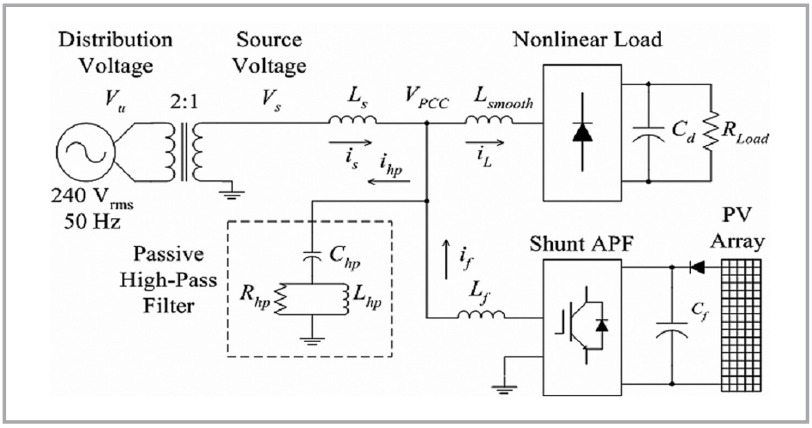

Figure 1(a): The proposed APF system

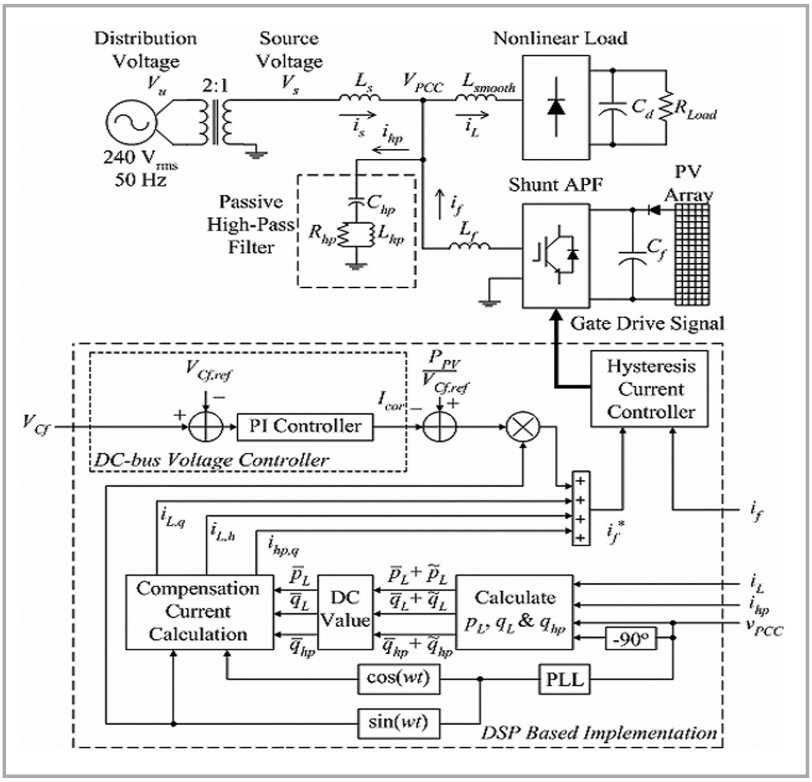

Figure 1(b): Overall system configuration and control block diagram

the passive HPF. It is envisaged that this configuration is effective to improve the filtering performance of high-order harmonics, thus achieving wideband harmonic compensation.

The VSI is operated in the current-controlled mode (CCM). Furthermore, the proposed hybrid APF with PV system is connected with the distribution line at the point of common coupling (PCC) through a filter inductor, allowing the reactive power control. Figure 1b shows the control system for the proposed hybrid APF with PV system. The compensated source current is desired to be sinusoidal to yield a maximum power factor (PF). The extension p-q theorem is introduced to derive the compensation current reference. Furthermore, a current must be drawn from the distribution source to maintain the voltage across the DC-bus capacitor to a value that is higher than the amplitude of the source voltage. A proportional-integral (PI) controller is implemented for the DC-bus capacitor voltage control. Under the normal operation, the PV array will provide active power to the load and the distribution. However, under no PV power generation condition, the distribution source supplies the active power to the load directly.

A.1 Derivation of Compensation Current Reference

Compensation current reference derivation for the single-phase two-wire APF based on extension p-q theorem has been presented in [14]. In this work, the application of the theorem is further extended to a single-phase two-wire hybrid APF with PV system. The compensation current reference derivation for the proposed scheme is presented in [17]. The extension p-q theorem is adopted for the derivation of active, reactive and harmonics components of nonlinear load current and the reactive component of passive HPF current.

For a single-phase two-wire system with nonlinear load, the load current can be represented as

$$i_L(t) = \sum_{n=1}^{\infty} \sqrt{2I_{L,n}} \sin(n\omega t + \theta n) \quad (1)$$

Under normal circumstances, the voltage at PCC can be assumed to be a sinusoidal, i.e.,

$$v_{PCC}(t) = \sqrt{2V_{PCC}} \sin(\omega t + \phi) \quad (2)$$

The HPF current can be represented as

$$i_{hp}(t) = \sqrt{2I_{hp,n}} \sin(\omega t + 90°) \quad (3)$$

Therefore, the instantaneous active power of nonlinear load can be calculated as

$$PL(t) = v_{PCC}(t).iL(t) = \bar{P}L + P\tilde{L} \quad (4)$$

The instantaneous reactive power of nonlinear load can be written as follows

$$q_L(t) = v'_{PCC}(t).i_{hp}(t) = \bar{q}_L + \tilde{q}_L \quad (5)$$

The instantaneous reactive power of HPF can be calculated as

$$q_{hp}(t) = v'_{PCC}(t).i_{hp}(t) = \bar{q}_{hp} + \tilde{q}_{hp}, \quad (6)$$

where $\bar{p}_L$, $\bar{q}_L$ and $\bar{p}_{hp}$ represent the constant part, $\tilde{p}_L$, $\tilde{q}_L$ and $\tilde{p}_{hp}$ denote the variant component, and $v'_{PCC}(t)$ denotes the PCC voltage shifted by 90°.

By obtaining the constant part in (4), (5) and (6), the active ($i_{L,p}$), reactive ($i_{L,q}$) and harmonics ($i_{L,h}$) components of nonlinear load current and the reactive ($i_{hp,q}$) component of the passive HPF current can be readily calculated as follows:

$$i_{L,p}(t) = \sqrt{2}\,\frac{\bar{p}_L}{V_{PCC}}\,u(t), \quad (7)$$

$$i_{L,q}(t) = \sqrt{2}\,\frac{\bar{q}_L}{V_{PCC}}\,u(t-90°), \quad (8)$$

$$i_{L,h}(t) = i_L(t) - i_{L,p}(t) - i_{L,q}(t), \quad (9)$$

and

$$i_{hp,q}(t) = \sqrt{2}\,\frac{\bar{q}_{hp}}{V_{PCC}}\,u(t-90^{\circ}), \tag{10a}$$

where $u(t)$ is a unit vector in phase with the PCC voltage.

Finally, the compensation current reference can be expressed as

$$i^{*}_{f} = i_{L,q} + i_{L,h} + i_{hp,q} - I_{Cf}\cdot u(t) + \frac{P_{PV}}{V_{Cf,\,ref}}\cdot u(t), \tag{10b}$$

where P_{PV} is the active power of PV array, I_{Cf} is the DC-bus capacitor charging current, and $V_{Cf,\,ref}$ is DC-bus capacitor voltage reference.

A2. DC-Bus Voltage Control

Under a loss free situation, the hybrid APF need not to provide any active power to cancel the reactive and harmonic currents from the load, and the reactive current from the HPF. These currents show up as reactive power. Thus, it is indeed possible to make the DC-bus capacitor to deliver the reactive power demanded by the proposed hybrid APF. As the reactive power comes from the DC-bus capacitor and this reactive energy transfer between the load and the DC-bus capacitor (charging and discharging of the DC-bus capacitor), the average DC-bus voltage can be maintained at a prescribed value.

However, due to switching loss, capacitor leakage current, etc., the distribution source must provide not only the active power required by the load but also the additional power required by the VSI to maintain the DC-bus voltage constant. Unless these losses are regulated, the DC-bus voltage will drop steadily.

A PI controller used to control the DC-bus voltage is shown in Figure 2. Its transfer function can be represented as

$$H(s) = K_p + \frac{K_I}{s} \tag{10b}$$

where K_p is the proportional constant that determines the dynamic response of the DC-bus voltage control, and K_I is the integration constant that determines its settling time.

It can be noted that if K_p and K_I are large, the DC-bus voltage regulation is dominant, and the steady-state DC-bus voltage error is low. On the hand, if K_p and K_I are small, the real power unbalance give little effect to the transient performance. Therefore, the proper selection of K_p and K_I is essentially important to satisfy above mentioned two control performances .

As described in [5], the K_p can be calculated using the energy-balance principle. After K_p is calculated, the K_I can be determined empirically. Appendix C presents the K_p calculation using the energy-balance principle for the proposed hybrid APF.

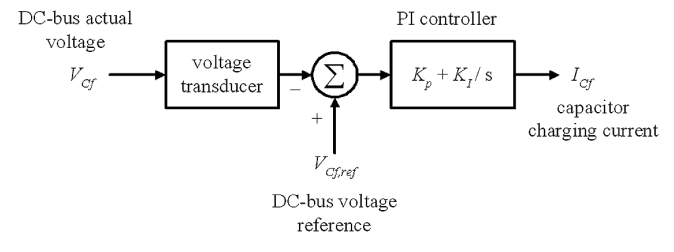

Figure 2: PI controller for DC-bus voltage control

B. Hysterisis Current Controller

In order to generate the compensation current that follows the current reference, the fixed-band hysteresis current control method is adopted. It imposes a bang-bang type instantaneous control that forces the APF compensation current (i_f) or voltage (v_f) signal to follow its estimated reference signal ($i_{f,\,ref}$ or $v_{f,\,ref}$) within a certain tolerance band. In this control scheme, a signal deviation (H) is designed and imposed on $i_{f,\,ref}$ or $v_{f,\,ref}$ to form the upper and lower limits of a hysteresis band. The i_f or v_f is then measured and compared with $i_{f,\,ref}$ or $v_{f,\,ref}$; the resulting error is subjected to a hysteresis controller to determine the gating signals when exceeds the upper or lower limits set by (estimated reference signal + H/2) or (estimated reference signal − H/2). As long as the error is within the hysteresis band, no switching action is taken. Switching occurs whenever the error hits the hysteresis band. The APF is therefore switched in such a way that the peak-to-peak compensation current/voltage signal is limited to a specified band determined by H as illustrated by Figure 3. Hysteresis current controller with a fixed H is implemented is known to be more popular. To obtain a compensation current (i_f) with switching ripples as small as possible, the value of H can be reduced. However, doing so results in higher switching frequency. Thus, increases losses on the switching transistors.

The advantages of using the hysteresis current controller are its excellent dynamic performance and controllability of the peak-to-peak current ripple within a specified hysteresis band. Furthermore, the implementation of this control scheme is simple. However, this control scheme exhibits several unsatisfactory features. The main drawback is that it produces uneven switching frequency. Consequently, difficulties arise in designing the passive HPF. Furthermore, there is possibly generation of unwanted resonances on the power distribution system. Besides, the irregular switching also affects the APF efficiency and reliability.

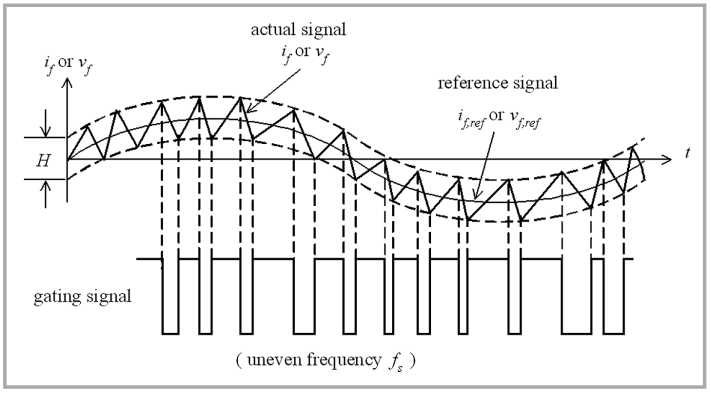

Figure 3: Gating signal generation by hysteresis controller

C. Design of Passive High-Pass Filter

The second-order damped series resonant type HPF topology is adopted in the proposed hybrid APF with PV system. The HPF consists of a capacitor C_{hp} , inductor L_{hp} and an inductor bypass resistor R_{hp}. Figure 3 presents an equivalent circuit of the proposed hybrid APF system for harmonics, where Z_{hp} is the equivalent impedance of HPF and Z_s is the equivalent source impedance assumed to be a simple inductor. In Figure 4, the shunt

APF is assumed to act as an ideal current source which produces the compensation current that follows the current reference, while the nonlinear load is considered as a harmonics current source. Since we are only interested in the system performance with the harmonics components, we can neglect the source voltage. This is because the source voltage is assumed to contain only the fundamental frequency component.

A generalised transfer function approach to harmonic filter design has been presented in [18]. This method is based on the Laplace transform and superposition. In this work, the transfer function approach to harmonic filter design is adopted for the passive HPF design. The HPF impedance transfer function can be derived in normalised form as

$$H_{hp}(s) = Z_{hp}(s) = \frac{A}{s\left(\frac{s}{\omega_p} + 1\right)} \cdot \left[\left(\frac{s}{\omega_o}\right)^2 + \frac{1}{Q}\left(\frac{s}{\omega_o}\right) + 1\right]. \quad (12)$$

In (12),

$$A = \frac{1}{C_{hp}}, \ \omega_o = \frac{1}{\sqrt{L_{hp} C_{hp}}}, \ \omega_p = \frac{R_{hp}}{C_{hp}}, \ Q = R_{hp}\sqrt{\frac{C_{hp}}{L_{hp}}},$$

where A is the gain coefficient, ω_o is the series resonant frequency, ω_p is the pole frequency, and Q is the quality factor.

The passive HPF is tuned to the resonant frequency of 1.28 kHz ($f_o = \frac{1}{2\pi\sqrt{L_{hp} C_{hp}}} = 1.28$ kHz). This resonant frequency value is chosen as the filtering performance of the APF is impaired above this frequency.

Depending on the value selected for the inductor bypass resistor R_{hp}, many different transfer function characteristics are possible. The inductor bypass resistor R_{hp} is chosen based on the desired high-pass response and the series resonant attenuation. The quality factors of $0.5 \leq Q \leq 2.0$ are typical. Higher Q factors allow more series resonant attenuation and less high-pass. By contrast, lower Q factors provide less series resonant attenuation and greater high-pass response. Hence, the proper selection of Q is essentially required to satisfy the series resonant and high-pass response performances. In this work, the Q factor was selected as 0.69, considering the required high-pass response over a wide frequency band.

After the hybrid APF with PV system is configured and $Z_{hp}(s)$ is known, the distribution system current to injected current transfer function $H_{cds}(s)$ can be derived for the hybrid APF with PV system connected to the PCC as

$$H_{cds}(s) = \frac{i_{s,h}(s)}{i_h(s)} = \frac{Z_{hp}(s)}{Z_{hp}(s) + Z_s(s)} \quad (13)$$

Transfer function (13) is important because it can be used to assess the overall system performance. A bode magnitude plot of is shown in Figure 5 where it has one crest due to the parallel resonance between $L_s + L_{hp}$ and C_{hp}. In particular, the parallel resonance is a problem, as it enlarges harmonics around the parallel resonant frequency ($f_r = \frac{1}{2\pi\sqrt{(L_s + L_{hp}) C_{hp}}} = 1.07$ kHz). This

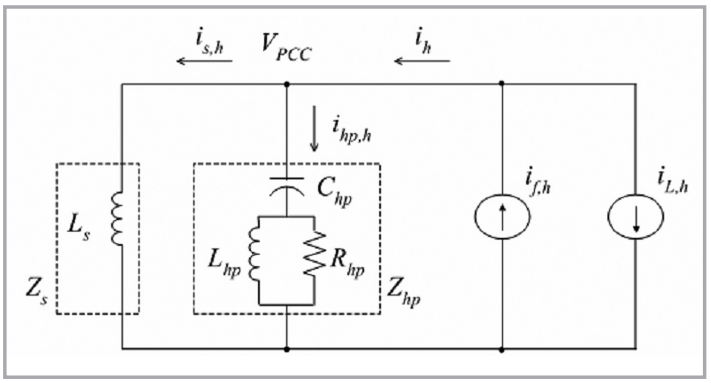

Figure 4: Simplified model of the hybrid filter

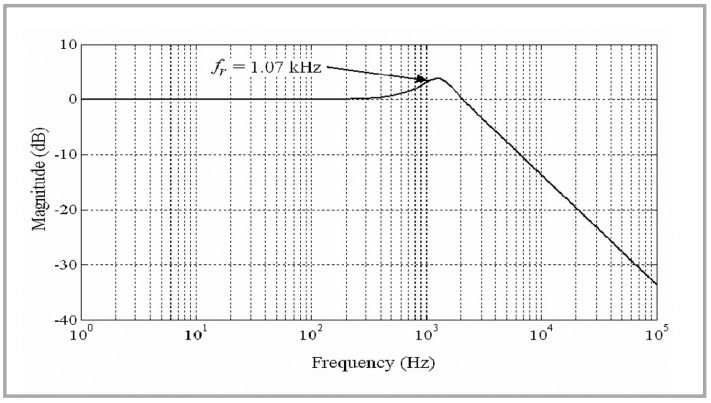

Figure 5: Bode magnitude diagram of the transfer function for the proposed hybrid APF system

crest can be minimised by selecting the value of Q factor close to 0.7. For the plot shown in Figure 4, the distribution system current to injected current transfer function $H_{cds}(s)$ can be evaluated at low and high frequencies. For low frequencies, it has a 0 dB gain from 0 Hz to the parallel resonant frequency f_r. At f_r the gain is determined by the selection of Q. For high frequencies, the roll-off of the high frequency components above the parallel resonant frequency f_r is -20 dB per decade. Hence, the harmonics filtering is divided between the two filters: the low-order harmonics are compensated using the shunt APF, while the high-order harmonics are filtered by the passive HPF.

III. EXPERIMENTAL RESULTS

The proposed hybrid APF system was tested in the laboratory with a 500W experimental prototype. An overall block diagram of the experimental set-up is shown in Figure 6. The heart of the overall control system is the dSPACE DS1104 DSP controller board which is programmed to realise the compensation current reference estimation and control algorithm. It is also used to generate the required gating signals to the VSI. Programming with C code is done using the dedicated ControlDesk Source Code Editor and Microtec PowerPC C Compiler and Linker. The executable object files and libraries are generated and loaded onto the on-board global memory for real-time execution. To maintain consistency throughout the experiment, a DC source is used along with the Voltage Source Inverter. However during the experiments involving PV power real PV arrays are used.

The system parameters are shown in Table 1. For the experimental system, the leakage impedance of the transformer is assumed to be the source impedance, L_s = 0.76 mH. The passive HPF is tuned to the resonant frequency of 1.28 kHz. The design parameters of the HPF are: L_{hp} = 1.76 mH, C_{hp} = 8.8 μF and

C_{hp} = 10 Ω . A diode rectifier with a DC-link capacitor C_d and a smoothing inductor L_{smooth} was used as the load.

The source current waveform and its harmonics spectra without compensation are shown in Figure 7. As can be seen, the source current is highly distorted, with very sharp peak and high crest factor. The measured total harmonics distortion measured up to 10KHz ($THD_{10\,kHz}$) is 130%.

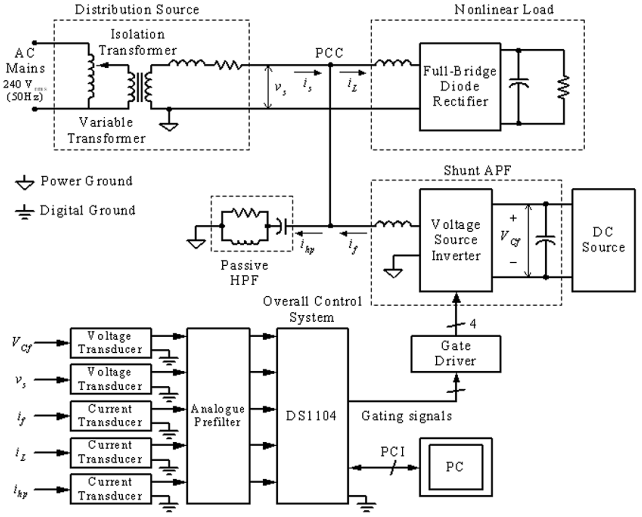

Figure 6: Overall block diagram of the experimental set-up of the proposed APF

Table 1: Experimental system parameters

Distribution Voltage	V_u = 240 V_{rms} (50Hz)
Source Inductance	L_s = 0.76 mH
Rectifier DC-link Capacitor	C_d = 1000 μF
Rectifier Smoothing Inductor	L_{smooth} = 1.15 mH
Maximum Switching Frequency	$f_{sw,\,max}$ = 10 kHz
Hysteresis Current Control Band	H = 1.0 $A_{peak\text{-}to\text{-}peak}$
APF Inductor	L_f = 10.0 mH
APF DC-bus Capacitor	C_f = 1000 μF
DC-bus Capacitor Voltage Reference	$V_{Cf,ref}$ = 250 V_{dc}
HPF Inductor	L_{hp} = 1.76 mH
HPF Capacitor	C_{hp} = 8.8 F
HPF Resistor	R_{hp} = 10 Ω
Load Resistor	R_L = 250 Ω

Table 2: Supply voltage harmonics without compensation

Harmonics	Magitude (V-peak)
Fundamental	350
3	15
5	7
7	3
9	1.2

Figure 8 presents the source current waveform with basic shunt APF. From the spectra, it can be observed that using the basic APF the source current is improved somewhat. It managed to retain its sinusoidal shape. However, contains appreciable amount of high-order harmonics. The measured $THD_{10\,kHz}$ is about 35%.

Figure 9 shows the performance of the system with the proposed scheme. As can be clearly seen, the source current is very near sinusoidal with $THD_{10\,kHz}$ about 2.5%. The results prove that the proposed APF is able to improve the performance of the basic APF significantly.

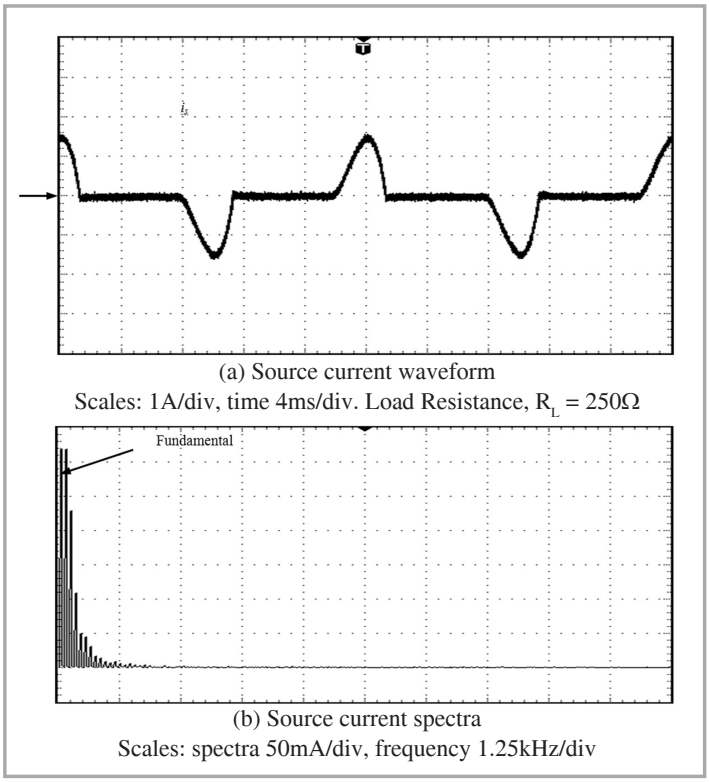

(a) Source current waveform
Scales: 1A/div, time 4ms/div. Load Resistance, R_L = 250Ω

(b) Source current spectra
Scales: spectra 50mA/div, frequency 1.25kHz/div

Figure 7: Source current without compensation

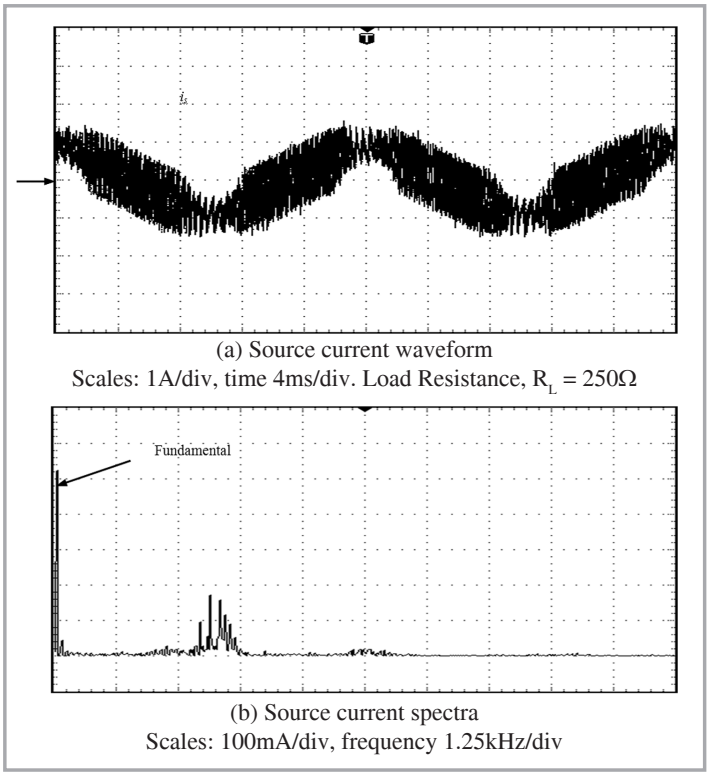

(a) Source current waveform
Scales: 1A/div, time 4ms/div. Load Resistance, R_L = 250Ω

(b) Source current spectra
Scales: 100mA/div, frequency 1.25kHz/div

Figure 8: Source current with basic shunt APF

The main currents in the proposed APF system are shown in Figure 10. By using extension p-q theorem presented in Section II, the compensation current reference can be decomposed into active, reactive and harmonic current components. Referring to Figure 10, it can be seen that the active load current ($i_{L,p}$) is in phase with the source voltage (V_s), while the reactive load current ($i_{L,p}$) lags $i_{L,p}$ by

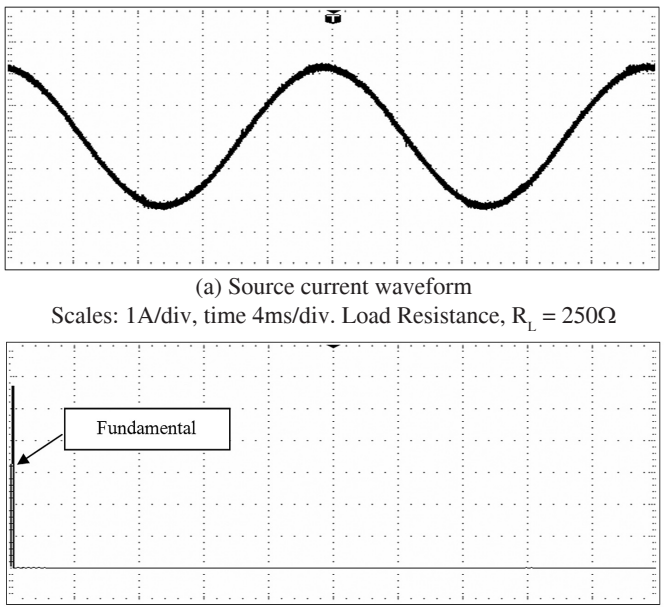

(a) Source current waveform
Scales: 1A/div, time 4ms/div. Load Resistance, $R_L = 250\Omega$

(b) Source current spectra
Scales: 100mA/div, frequency 1.25kHz/div

Figure 9: Source current with proposed APF scheme.

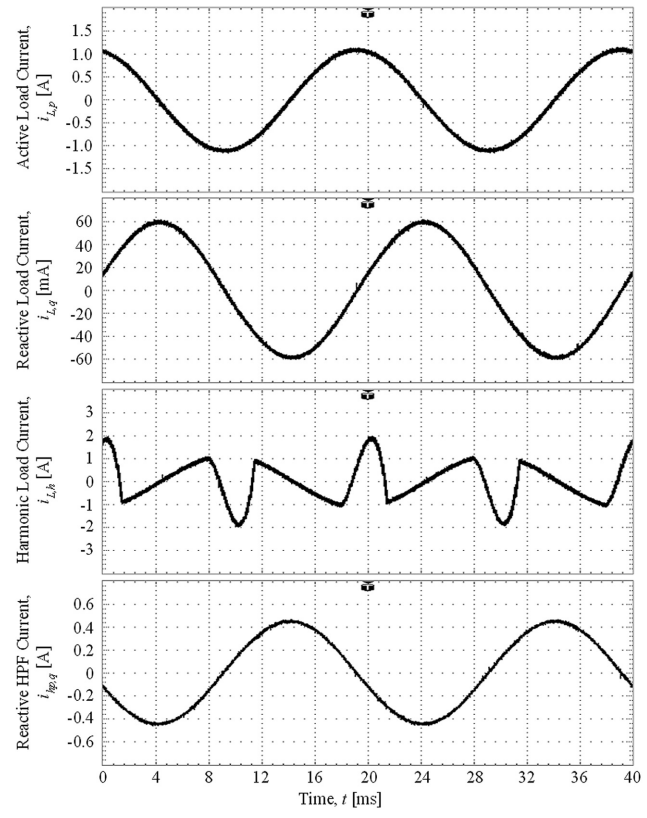

Figure 10: Key currents in the proposed APF scheme

90°. The harmonic load current ($i_{L,h}$) is obtained by subtracting $i_{L,p}$ and $i_{L,q}$ from the load current (i_L), i.e. $i_{L,h} = i_L - (i_{L,p} + i_{L,q})$. In addition, this figure also shows the reactive HPF ($i_{hp,q}$) current waveform. It is in phase with the HPF current (i_{hp}).

Figure 11 shows the supply voltage distortion due the non-sinusoidal load current. Without any compensation, it can be seen that the supply voltage appears to exhibit the "flat-top" phenomena. It implies that that the voltage has very low order harmonics, i.e the

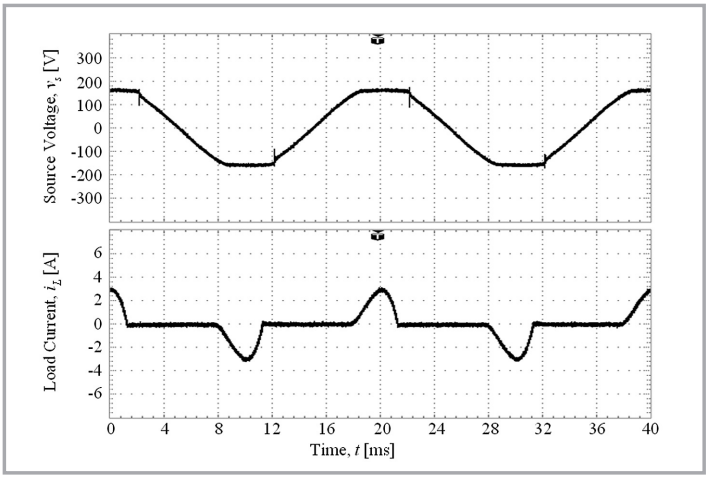

Figure 11: Supply voltage and load current without compensation

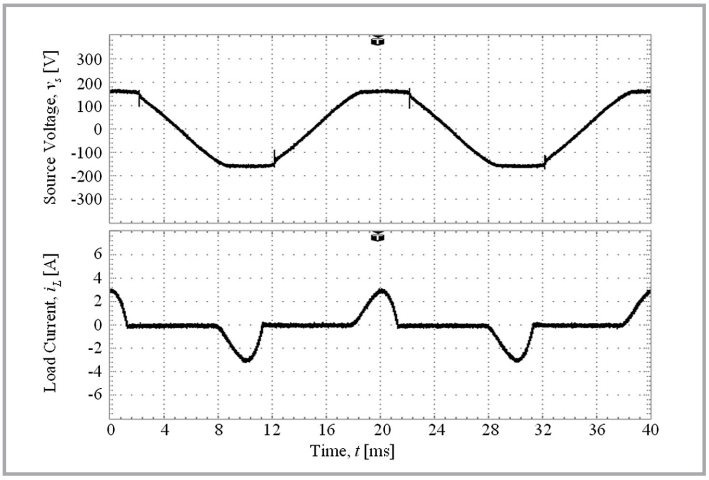

Figure 11: Supply voltage and load current without compensation

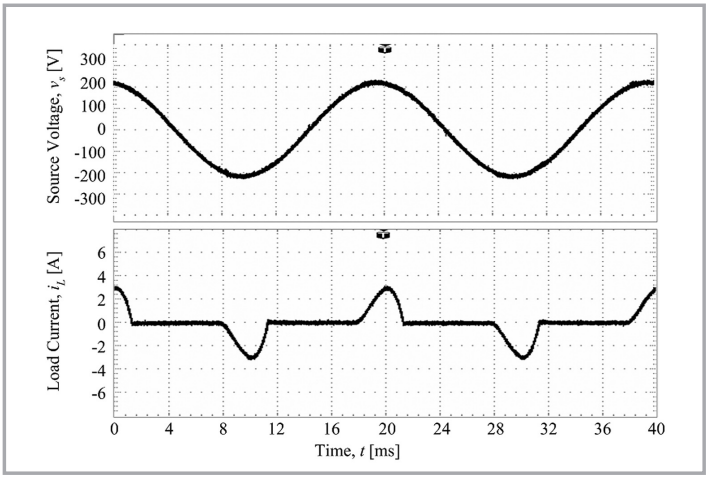

Figure 12: Supply voltage and load current with the proposed APF

3rd, 5th etc. These harmonics are extremely difficult to filter. The measured voltage harmonics are tabulated in Table 2.

Figure 12 shows the supply voltage waveform with the same loading conditions, but with the proposed APF applied. As can be observed, the flat-top has vanished from the waveform. It is very close to sinusoidal with THD of about 2%.

Figure 13(a) shows the load current and compensated source current waveforms with no active power generation from PV array. The active power is provided by the distribution line directly. Figure 13(b) shows the load current and compensated source current waveforms with 175 W active power generation from PV

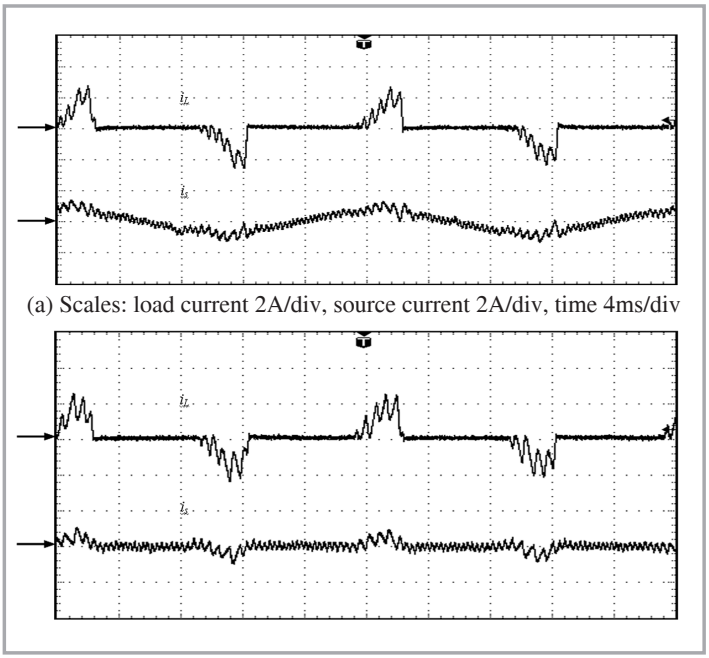

(a) Scales: load current 2A/div, source current 2A/div, time 4ms/div

(b) Scales: load current 2A/div, source current 2A/div, time 4ms/div

Figure 13: Experimental results with proposed APF with PV system (a) load and source current waveforms with no PV power generation and (b) load and source current waveforms with 175 W PV power generation

array. The experimental results obtained show that the generated PV power is provided to the load and distribution through the proposed hybrid APF system.

IV. CONCLUSIONS

A single-phase two-wire hybrid APF that interconnects to the PV system is presented. The proposed scheme combines the APF with a passive filter to improve the filtering performance of high-order harmonics. The derivation of compensation current reference is simpler with the utilisation of extension p-q theorem. The experimental results show the effectiveness of the proposed scheme for wideband harmonics compensation and PV power handling capability. ■

APPENDIX A:

PROPORTIONAL CONSTANT (K_p) CALCULATION USING ENERGY-BALANCE PRINCIPLE

The proportional constant (K_p) calculation using the energy-balance principle is proposed by Hsu, C. Y. [5]. In this work, the energy-balance principle is adopted for K_p calculation. After K_p is calculated, the integration constant (K_I) can be determined using empirical method. The K_p calculation based energy-balance principle for the proposed hybrid APF is described as in the following.

If the reference voltage across the DC-bus capacitor is $V_{Cf,ref}$, then the reference energy in the capacitor will be

$$E_{Cf,ref} = \frac{1}{2} C_f V^2_{Cf,ref} \quad \text{(A.1)}$$

while the instantaneous energy in the capacitor is

$$E_{Cf}(t) = \frac{1}{2} C_f V^2_{Cf,ref}(t) \quad \text{(A.2)}$$

Therefore, the energy loss of the capacitor in one cycle is

$$\Delta E_{Cf}(t) = E_{Cf,ref} - E_{Cf}(t)$$

$$= \frac{C_f}{2} [\, V^2_{Cf,ref} - v^2_{Cf}(t) \,]$$

$$= \frac{C_f}{2} [\, V_{Cf,ref} + v_{Cf}(t) \,][\, V_{Cf,ref} - v_{Cf}(t) \,] \quad \text{(A.3)}$$

Assume that the variation in DC-bus voltage within one cycle is moderate, the term $[\, V_{Cf,ref} + v_{Cf}(t) \,]$ can be approximated as

$$V_{Cf,ref} + v_{Cf}(t) \approx 2V_{Cf,ref} \quad \text{(A.4)}$$

$$\Delta E_{Cf}(t) = C_f V_{Cf,\,ref} [\, V_{Cf,ref} - v_{Cf}(t) \,] \quad \text{(A.5)}$$

Since this energy loss must be supplied by the distribution source, the peak value of the DC-bus capacitor charging current (I_{Cf}) can be estimated as follows:

$$\int_o^T \sqrt{2V_s} \sin(\omega t)\, I_{Cf} \sin(\omega t) dt = \Delta \mathrm{E_{Cf}} \quad \text{(A.6)}$$

Therefore

$$I_{Cf} = \frac{2}{T\sqrt{2\mathrm{V_s}}} \Delta \mathrm{E_{Cf}}$$

Substituting (A.5) into (A.7) gives

$$I_{Cf} = \frac{2}{T\sqrt{2\mathrm{V_s}}} C_f V_{Cf,\,ref} [\, V_{Cf,ref} - v_{Cf}(t) \,]$$

$$= \frac{2\, C_f V_{Cf,\,ref}}{T\sqrt{2\mathrm{V_s}}} [\, V_{Cf,ref} - v_{Cf}(t) \,]$$

$$= K_p [\, V_{Cf,ref} - v_{Cf}(t) \,] \quad \text{(A.8)}$$

where the proportional constant (K_p) is given by

$$K_p = \frac{2\, C_f V_{Cf,\,ref}}{T\sqrt{2\mathrm{V_s}}} \quad \text{(A.9)}$$

REFERENCES

[1] H. Akagi, "New trends in active filters for power conditioning," IEEE Trans. on Industry Applications, vol. 32, no. 6, pp. 1312-1322, Nov.-Dec. 1996.

[2] D. Sutanto, M. Bou-rabee, K. S. Tam, and C. S. Chang, "Harmonic filters for industrial power systems," in Proc. IEE International Conference on Advances in Power System Control, Operation and Management, APSCOM, 1991, Hong Kong, vol. 2, pp. 594-598.

[3] J. C. Das, "Passive filters – potentialities and limitations," IEEE Trans. on Industry Applications, vol. 40, no.1, pp. 232-241, Jan.-Feb. 2004.

[4] H. L. Jou, J. C. Wu, and H. Y. Chu, "New single-phase active power filter," in Proc. IEE Electric Power Applications, vol. 141, no. 3, pp. 129-134, May 1994.

[5] C. Y. Hsu, and H. –Y. Wu, "A new single-phase active power filter with reduced energy-storage capacity," in Proc. IEE Electric Power Applications, vol. 143, no. 1, pp. 25-30, Jan. 1996.

[6] S. G. Jeong and M. H. Woo, "DSP-based active power filter with predictive current control," IEEE Trans. on Industrial Electronics, vol. 44, no. 3, pp. 329-336, June 1997.

[7] S. Buso, L. Malesani, P. Mattavelli, and R. Veronese, "Design and fully digital control of parallel active power filters for thyristor rectifiers to comply with IEC-1000-3-2 standards," IEEE Trans. on Industry Applications, vol. 34, no. 3, pp. 508-517, May-June 1998.

[8] S. Fukuda and T. Endoh, "Control method for a combined active filter system employing a current source converter and a high pass filter," IEEE Trans. on Industry Applications, vol. 31, no. 3, pp. 590-597, May-June 1995.

[9] S. Khositkasame and S. Sangwongwanich, "Design of harmonic current detector and stability analysis of a hybrid parallel active filter," in Proc. Power Conversion Conference, PCC, 1997, Nagaoka, Japan, vol. 1, pp. 181-186.

[10] M. Routimo, M. Salo, and H. Tuusa, "A novel control method for wideband harmonic compensation," in Proc. IEEE International Conference on Power Electronics and Drive Systems, PEDS, 2003, Singapore, vol. 1, pp. 799-804.

[11] S. R. Bull, "Renewable energy today and tomorrow," in Proc. of the IEEE, vol. 89, no. 8, pp. 1216-1226, Aug. 2001.

[12] S. Kim, G. Yoo, and J. Song, "A bifunctional utility connected photovoltaic system with power factor correction and U.P.S. facility," in Proc. IEEE Photovoltaic Specialist Conference, 1996, Washington, USA, pp. 1363-1368.

[13] Y. Komatsu, "Application of the extension pq theory to a mains-coupled photovoltaic system," in Proc. Power Conversion Conference, PCC, 2002, Osaka, Japan, vol. 2, pp. 816-821.

[14] T. –F. Wu, C. –L. Shen, C. H. Chang, and J. –Y. Chiu, "1/spl phi/ 3W grid-connection PV power inverter with partial active power filter," IEEE Trans. on Aerospace and Electronic Systems, vol. 39, no. 2, pp. 635-646, April 2003.

[15] Y. Komatsu and T. Kawabata, "Characteristics of three phase active power filter using extension pq theory," in Proc. IEEE International Symposium on Industrial Electronics, ISIE, 1997, Guimaraes, Portugal, vol. 2, pp. 302-307.

[16] B. Dobrucky, H. Kim, V. Racek, M. Roch, and M. Pokorny, "Single-phase power active filter and compensator using instantaneous reactive power method," in Proc. Power Conversion Conference, PCC, 2002, Osaka, Japan, vol. 1, pp. 167-171.

[17] P. C. Tan and Z. Salam, "A new single-phase two-wire hybrid active power filter using extension p-q theorem for photovoltaic application," in Proc. National Power and Energy Conference, PECon, 2004, Malaysia, pp. 126-131.

[18] J. K. Phipps, "A transfer function approach to harmonic filter design," IEEE Industry Applications Magazine, vol. 3, no. 2, pp. 68-82, Mar.-Apr. 1997.

PROFILES

DR ZAINAL SALAM

Dr Zainal Salam was born in Seremban, Malaysia in 1963. He received his secondary education from Victoria Institution, Kuala Lumpur. He obtained his B.Sc., M.E.E. and Ph.D. from the University of California, UTM and University of Birmingham, UK, in 1985, 1989 and 1997, respectively. He has been a lecturer at UTM for 21 years and is currently an Associate Professor at the Department of Energy Conversion Department. For the past ten years he has been working on 20 researches and consulting projects with various companies and agencies such as MOSTI, PTM, UNDP, SIRIM and Grand Battery Technologies. Currently he serves as the Director of the Inverter Quality Control Center, UTM, specializing on testing and failure analysis of photovoltaic inverters. He has written over 80 articles published in various journals and conferences. His research interests include all areas of power electronics. Currently, he is involved in several e-Science projects in the area of renewable energy, power electronics and machine control.

TAN PERNG CHENG

Tan Perng Cheng was born in Johor, Malaysia in 1980. He received the B.Sc and MEng degrees in electrical engineering from Universiti Teknologi Malaysia (UTM), Johor, Malaysia, in 2003 and 2006, respectively. He is currently working with a power quality (PQ) solution company in Singapore. His research interests are the areas of active power filters, power electronics, and renewable energy.

AWANG JUSOH

Awang Jusoh was born in Terengganu, Malaysia in 1964. He received his B.Sc. from the Brighton Ploy, UK, in 1988. He obtained his M.Sc. and Ph.D. from the University of Birmingham, UK, in 1995 and 2004, respectively. He is currently a senior lecturer at the Department of Energy Conversion, Faculty of Electrical Engineering, UTM, Malaysia. His research interests are the areas of modeling, analysis and control of power electronic systems.